Influence of Mistuning on Rotor-Blade Vibrations

L. E. EL-BAYOUMY*
Consultants & Designers, Inc., East Hartford, Conn.
AND
A. V. SRINIVASAN†
Pratt & Whitney Aircraft, United Aircraft Corporation, East Hartford, Conn.

This analysis is aimed at determining the influence of blade mistuning on the vibratory stress levels of turbine and compressor blades. A frequency response analysis for a given rotor configuration shows that a large number of resonances may occur over a frequency band, the width of which is nearly 20% of the mean blade frequency. The resonant amplitudes are a function of blade frequency and location on the rotor, and the amount of damping present in the system. A parametric study is carried out to evaluate the response levels due to engine order excitation, aerodynamic and mechanical damping, and blade frequency deviation. The resulting mode shapes and frequencies are in good agreement with the experimental findings reported earlier in the literature.

Nomenclature

a_{kl}, b_{kl} = coefficients defined in Eqs. (11)
C^a = coefficient of aerodynamic damping
C^m = coefficient of mechanical damping
F = amplitude of $f(t)$
$f(t)$ = dynamic force transmitted to the disk
$\mathcal{F}$ = defined in Eq. (11)
$\bar{F}$ = $(\mathcal{F}^2+\mathcal{G}^2)^{1/2}$
$\mathcal{G}$ = defined in Eq. (11)
K = blade stiffness
M = blade mass
N = number of blades mounted on the rotor
n = engine order of excitation
P = amplitude of exciting force
$p(t)$ = exciting force
$\mathcal{P}$ = defined in Eqs. (11)
$\bar{P}$ = $(\mathcal{P}^2+\mathcal{Q}^2)^{1/2}$
$\mathcal{Q}$ = defined in Eqs. (11)
t = time variable
W = disk rim amplitude
$w(t)$ = disk rim displacement
Y = blade amplitude
$y(t)$ = blade displacement
α_{kl} = disk rim receptances (dynamic influence coefficients)
$\bar{\alpha}_{kl}$ = dimensionless receptances, defined in Eqs. (11)
ζ = damping factor
ϕ = phase angle associated with exciting force
$\bar{\phi}$ = phase angle associated with disk displacement
χ = phase angle associated with transmitted force
ψ = phase angle associated with blade displacement
ω = frequency of excitation
ω_k = blade bench frequency

Subscripts
k, l, m = blade number or location around the disk

Introduction

TO insure the safe operation of modern turbomachine units, it has become essential to evaluate their response to vibratory loading conditions. This entails determination of natural frequencies and resonant amplitudes of the system. For bladed disks, it has been customary to assume that the blades of a given rotor have identical frequencies. Results based on such an assumption would indicate that under an excitation of a given engine order, all blades experience the same vibratory stress. However, experimental investigations[1-3] have shown that large variations could exist in stress amplitudes of the different blades on the same rotor. Such variations may originate from differences in blade frequencies commonly known as blade mistuning. These differences are unavoidable in practice because of machining tolerances and/or different end fixities. The problem is basically similar to the classical "tuned absorber" phenomenon in which part of a system (the absorber) may be resonating, while another part (the main system) may remain stationary. This results in a situation in which some blades on the rotor can experience stress amplitudes in excess of those for a corresponding tuned system.

The vibratory behavior of a bladed disk is further complicated by coupling between different blades on the same disk either mechanically through the disk, shrouds, and any interblade dampers, or aerodynamically through the airstream. The case of aerodynamic coupling was treated by Whitehead,[4] who modeled the blades as a number of oscillators coupled only through the aerodynamic forces. Other models, shown in Figs. 1 and 2, were used by Wagner,[1] and Dye and Henry,[2] to simulate mechanical coupling. The degree of predicted stress escalation due to mistuning varied from one author to another—understandably, because of the different models used.

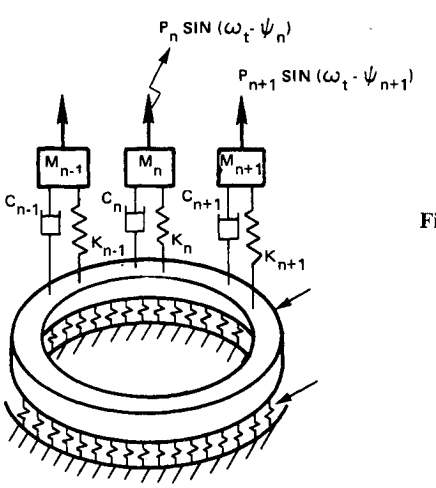

Fig. 1 Wagner's model.

Received February 27, 1974; revision received August 5, 1974.
Index categories: Aircraft Powerplant Design and Installation; Structural Dynamic Analysis.
* Advanced Vibration Analyst. Member AIAA.
† Senior Assistant Project Engineer, Technical & Research Section.

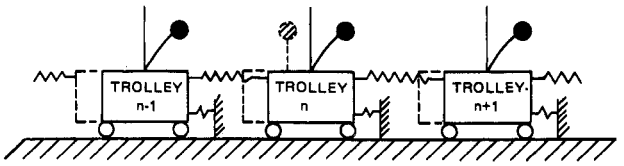

Fig. 2 Dye and Henry's model.

Ewins[3] has noted that detuning in a bladed disk may cause an n diametral mode to split into two modes with the same number of nodal diameters but with slightly differing frequencies, the difference being of the same order of magnitude as the maximum deviation in blade frequencies. In comparing the theoretically determined modes and frequencies for a 24-bladed wheel with those measured experimentally, Ewins[5] has shown that qualitative agreement in terms of blade amplitude patterns can be ascertained. The first four modes were recognized as the two- and three-nodal diameter "double modes," and the remaining modes did not possess any predominant diametral shape. About 10% discrepancy between theory and experiment was noted in the values of the first natural frequencies. It is probable that numerical approximations in evaluating disk receptances may have been responsible for much of this discrepancy. The predicted frequencies of the lower modes for the disk alone were over 20% off the experimental values.

The object of the present paper is to develop an alternate model based on treating the disk as an axisymmetric plate of variable thickness and by replacing each blade by a single-degree-of-freedom oscillator. To represent the damping present in the system, two dashpots are introduced, one connecting the blade to ground simulating aerodynamic damping and the other between the blade and the disk simulates mechanical damping. The blades in Ref. 5 are modeled as cantilever beams whose lengths vary according to the measured mistune distribution. Because the exact origin of mistuning cannot always be ascertained, a blade model consisting of a one degree-of-freedom system with a generalized mass and a stiffness equivalent to those of the actual blade may be adequate. Accurate values of the receptances of the disk are evaluated by means of the Myklestad approach. The 24-bladed rotor of Ref. 5 has been chosen as the example for an in-depth study using the present analysis. The actual measured distribution of blade frequencies, presented in Ref. 5, is used, as well as a series of periodic distributions in which the number of blades per pack is changed. First the mode shapes and natural frequencies are determined, then a frequency response analysis is carried out for various engine orders. The influence of damping on the response levels is evaluated by using appropriate values for the damping coefficients.

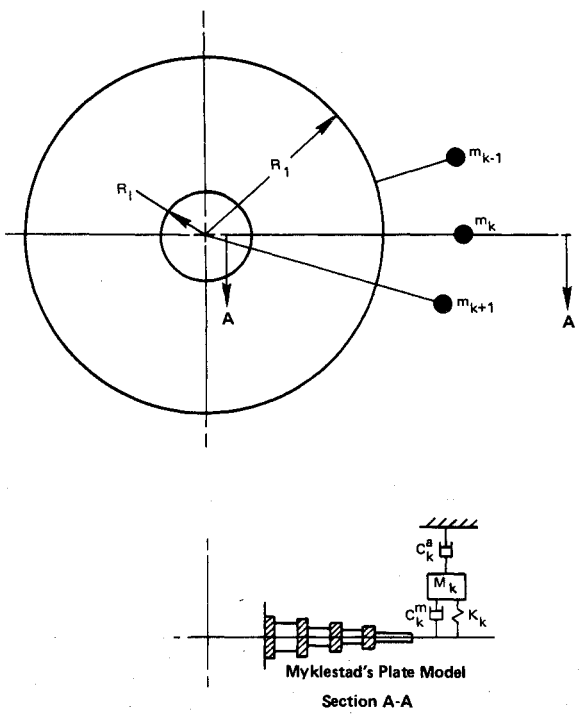

Fig. 3 Present model.

Derivation of Governing Equations

Consider a typical blade station whose model representation is shown in Fig. 3. Let θ_k denote the angular position of the blade, $w_k(t)$ the associated disk displacement, and $y_k(t)$ the blade displacement. Then, we may write the governing equation of motion as:

$$M_k \ddot{y}_k + C_k{}^a \dot{y}_k + K_k(y_k - w_k) + C_k{}^m(\dot{y}_k - \dot{w}_k) = P_k(t) \tag{1}$$

where

$$p_k(t) = P_k \exp i(\omega t + \phi_k) \tag{2}$$

The steady-state solution of Eq. (1) may likewise be expressed as follows:

$$y_k(t) = Y_k e^{i(\omega t + \psi_k)} \tag{3}$$

$$w_k(t) = W_k e^{i(\omega t + \bar{\phi}_k)} \tag{4}$$

where ψ_k and $\bar{\phi}_k$ are the phase angles associated with y_k and w_k and measured from the force acting on the reference blade.

Substitution of Eqs. (2–4) into Eq. (1) yields

$$[-M_k\omega^2 + i\omega(C_k{}^a + C_k{}^m) + K_k]Y_k e^{i\psi_k} - (K_k + iC_k{}^m\omega)W_k e^{i\bar{\phi}_k} = P_k e^{i\phi_k}$$
$$k = 1, 2, \ldots, N \tag{5}$$

The phase angle ϕ_k associated with a fluctuating gas stream is given by

$$\phi_k = 2\pi n(k-1)/N \tag{6}$$

where n is the engine order of excitation and N is the number of blades. If the dynamic force transmitted to the disk by the kth blade is denoted by $f_k(t) = F_k \exp i(\omega t + \chi_k)$, then the displacement of the disk, as a sum of contribution of all forces, can be stated as

$$w_k(t) = \sum_{l=1}^{N} \alpha_{kl} F_l e^{i(\omega t + \chi_l)} \tag{7}$$

In Eq. (7) α_{kl} denotes the amplitude at Station k of the disk, due to a force of unit amplitude applied at Station l. The coefficients α_{kl} are known as the dynamic influence coefficients, or the receptances of the disk. They are functions of disk geometry, material properties, boundary conditions, rotating speed, frequency of excitation, and blade positions θ_k and θ_l.

Since the force $f_k(t)$ is transmitted to the disk through the spring K_k and the dashpot $C_k{}^m$ it follows that

$$F_k e^{i\chi_k} = (i\omega C_k{}^m + K_k)(Y_k e^{i\psi_k} - W_k e^{i\bar{\phi}_k}) \tag{8}$$

Substituting Eqs. (7) and (8) and rearranging, we have

$$Y_k = \frac{F_k}{K_k + i\omega C_k{}^m} e^{i(\chi_k - \psi_k)} + \sum_{l=1}^{N} \alpha_{kl} F_l e^{i(\chi_l - \psi_k)} \tag{9}$$

Equation (5) can be reduced now to a set of N complex equations in the unknowns F_k and χ_k, $k = 1, 2, \ldots, N$. In terms of dimensionless components $\mathcal{F}_k$ and $\mathcal{G}_k$ of F_k the real and imaginary parts of this set becomes

$$\sum_{l=1}^{N} a_{kl}\mathcal{F}_l + \sum_{l=1}^{N} b_{kl}\mathcal{G}_l = \mathcal{P}_k$$

$$-\sum_{l=1}^{N} b_{kl}\mathcal{F}_l + \sum_{l=1}^{N} a_{kl}\mathcal{G}_l = \mathcal{Q}_k$$

$$k = 1, 2, \ldots, N \tag{10}$$

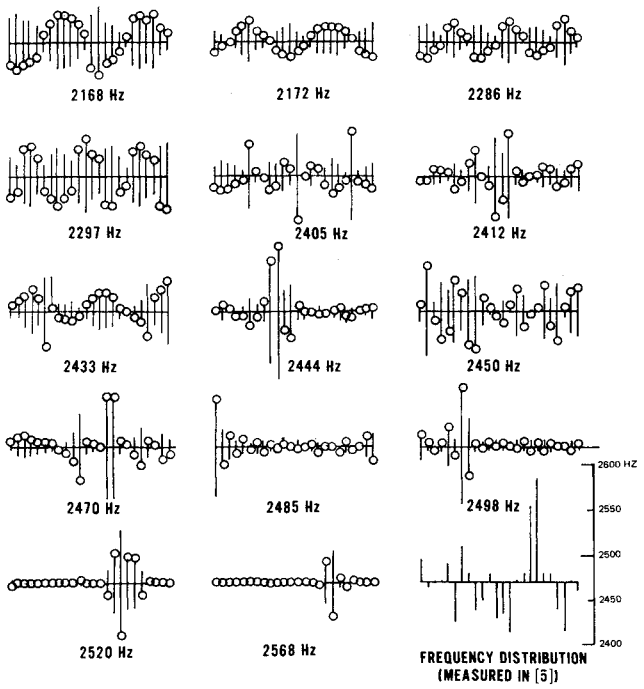

Fig. 4 Computed mode shapes for 24-bladed rotor with measured frequency distribution.

where

$$a_{kl} = [\omega_k{}^2(\omega_k{}^2-\omega^2)+4\zeta_{mk}(\zeta_{mk}+\zeta_{ak})\omega^2\omega_k{}^2]\delta_{kl} - \omega_k{}^2(\omega_k{}^2+4\zeta_{mk}{}^2\omega^2)\bar{\alpha}_{kl} \quad (11a)$$

$$b_{kl} = -2\omega_k\omega[\omega_k{}^2(\zeta_{mk}+\zeta_{ak})-\zeta_{mk}(\omega_k{}^2-\omega^2)]\delta_{kl} - 2\zeta_{ak}\omega_k{}^3(\omega_k{}^2+4\zeta_{mk}{}^2\omega^2)\bar{\alpha}_{kl}/\omega \quad (11b)$$

$$\omega_k{}^2 = K_k/M_k \quad (11c)$$

$$\bar{\alpha}_{kl} = M_k\omega^2\alpha_{kl} \quad (11d)$$

$$\zeta_{mk} = C_k{}^m/(4K_kM_k)^{1/2} \quad (11e)$$

$$\zeta_{ak} = C_k{}^a/(4K_kM_k)^{1/2} \quad (11f)$$

$$\mathscr{P}_k = (\omega_k{}^4+4\zeta_{mk}{}^2\omega^2\omega_k{}^2)P_k\cos(\phi_k)/P_1 \quad (11g)$$

$$\mathscr{Q}_k = (\omega_k{}^4+4\zeta_{mk}{}^2\omega^2\omega_k{}^2)P_k\sin(\phi_k)/P_1 \quad (11h)$$

$$\mathscr{F}_k = F_k\cos(\chi_k)/P_1 \quad (11i)$$

$$\mathscr{G}_k = F_k\sin(\chi_k)/P_1 \quad (11j)$$

Once Eqs. (10) are solved for $\mathscr{F}_k$ and $\mathscr{G}_k$ disk and blade amplitudes and phase angles can be calculated from Eqs. (7) and (9). In the particular case, when all blades are identical and P_k's are all the same, it can be shown that

$$\chi_1 = \arctan\frac{\sum_{k=1}^{N}(b_{1k}\cos\phi_k - a_{1k}\sin\phi_k)}{\sum_{k=1}^{N}(a_{1k}\cos\phi_k + b_{1k}\sin\phi_k)} \quad (12)$$

$$\chi_n = \chi_1+\phi_n \qquad n = 2,3,\ldots,N \quad (13)$$

$$\bar{F}_k = (\mathscr{F}_k{}^2+\mathscr{G}_k{}^2)^{1/2} \equiv \bar{F} = \bar{P}\Big/\sum_{k=1}^{N}[a_{1k}\cos(\chi_1+\phi_k)+b_{1k}\sin(\chi_1+\phi_k)] \quad (14)$$

Vibration Analysis of a Mistuned 24-Bladed Rotor

In this section, the response levels, natural frequencies, and mode shapes are determined for the example problem having primarily two different mistuning distributions: 1) a measured distribution used in Ref. 5, and 2) a square periodic distribution in which the pack size (a group of blades with identical frequency) is varied. The results pertaining to the two distributions are described in the following:

Mistune Distribution as Measured by Ewins[5]

This distribution is shown in Fig. 4. A comparison between the natural frequencies computed with the present model with those determined experimentally and analytically in Ref. 5 is shown in Table 1. As can be seen from the table, the present values are within 5% from the experimental results. The determined modes display the same features noted experimentally in Ref. 5; i.e., the first few modes possess a predominant diametral component while the rest are composed of several diametral components. In the last few modes only a small number of blades have noticable vibratory amplitudes.

Table 1 Natural frequencies of a 24-bladed rotor

Experimental (Ref. 5)	Analytical[a] (Ref. 5)	Present analysis
2037	1838.6	2168
2067	1847.8	2172
2300	2168.5	2286
2313	2178.7	2297
2340	2253.6	2405
2343	2271.7	2412
2368	...	2433
...	2307.4	2450
2382	2318.2	...
2388	2323.8	2470
2391	2342.1	2498
2394	2366.6	2485
2429	2388.5	2520
2478	2448.8	2568

[a] See corresponding mode shapes in Fig. 4.

The response of the given rotor to a 6EO (sixth engine order) excitation is plotted in Fig. 5 for three blades whose frequencies are the lowest, mean, and the highest. As can be seen, all the modes of the rotor wheel are excited by 6EO since a Fourier expansion of each mode would show a non-zero sixth order component. The intensity of such component varies in each mode as shown in Fig. 4 and is significantly large for modes in the neighborhood of the resonant frequency of the tuned rotor. It may be noted that the low-frequency blades suffer the highest level of stressing at an excitation frequency lower than the tuned rotor frequency and vice versa.

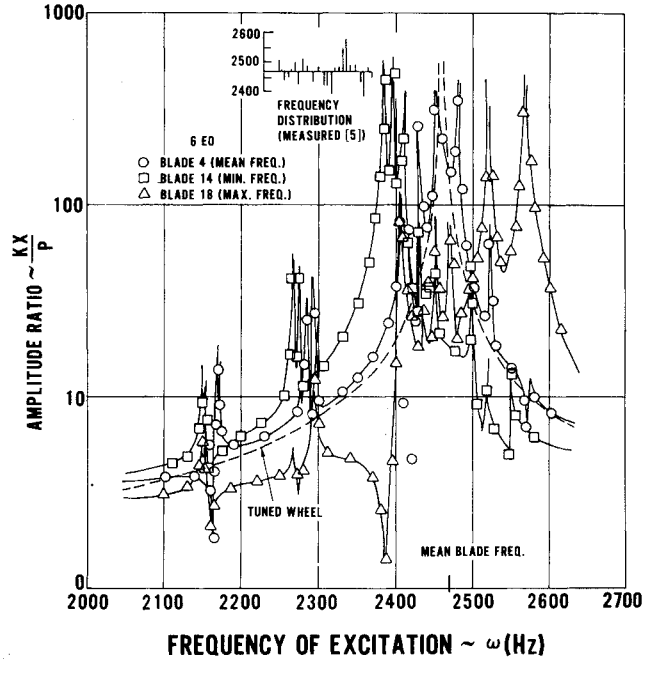

Fig. 5 Frequency response of a 24-bladed rotor.

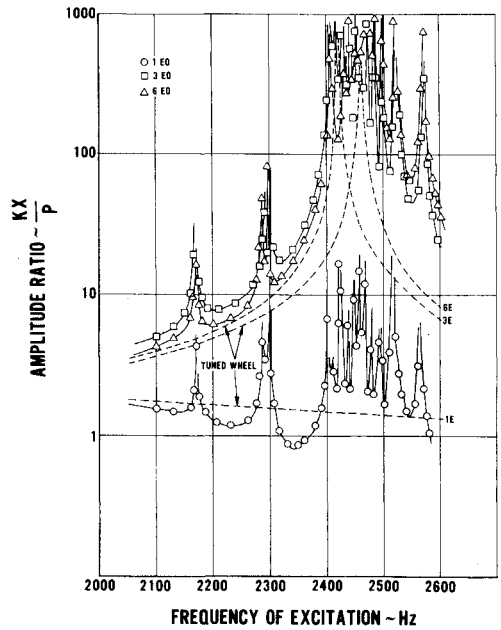

Fig. 6 Upper envelopes of the response levels for 24-bladed rotor with measured frequency distribution.

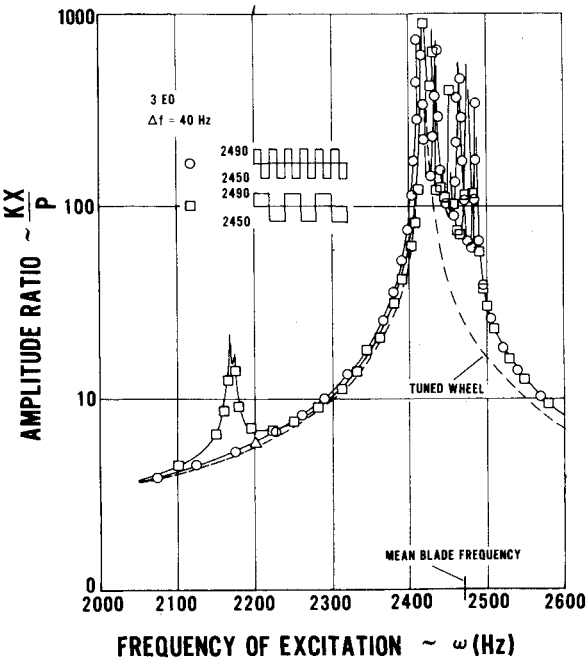

Fig. 8 Influence of pack size on the response levels of 24-bladed rotor with square distribution.

Blade 4, which has a bench frequency equal to the mean blade frequency, suffers a maximum stress level near the tuned system frequency. The tuned absorber behavior is well illustrated in Fig. 5; i.e., while blade 14 may be resonating, blade 18 is almost stationary.

As other engine orders may also be present in a general excitation, a frequency response diagram is plotted in Fig. 6 for engine orders 1, 3, and 6. In contrast to Fig. 5, the curves shown in Fig. 6 do not represent a particular blade, but rather the upper envelope of all blade responses for the given order of excitation. The resonant peaks in any engine order are experienced at the natural frequencies of the bladed rotor. This is significant because in experimental investigation, it suffices to excite the rotor in one engine order to obtain its resonant frequencies. In comparison with the response levels of the tuned rotor, drawn as dashed lines in Fig. 6, there is a marked difference in the first engine order. It should be noted that while a tuned wheel in 1EO does not suffer any resonances, the detuned rotor goes through the same number of resonances as for higher engine orders.

The influence of mechanical damping on the response levels is illustrated in Fig. 7. The upper envelope and the response of the critically stressed blade (No. 10) are compared to the response of the tuned wheel. Several observations are worth noting: 1) There is a 48% of overstressing in the detuned wheel. 2) Amplitudes at frequencies sufficiently far from the tuned system frequency are considerably lower than the maximum amplitude; 3) The frequency of the critically stressed blade (No. 10) does not represent the extreme mistune (see Fig. 4). 4) The resonant amplitudes of the detuned system are at least equal to that of the tuned system within a band width of about 145 Hz (see Fig. 7). It may be noted that this band width is of the same order of magnitude as the system mistune (170 Hz). The influence of aerodynamic damping is very similar

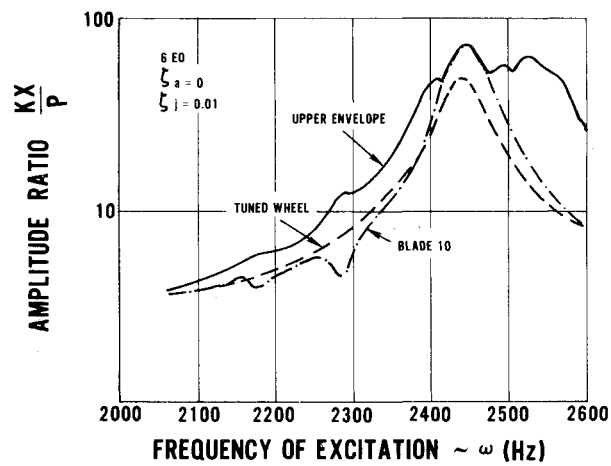

Fig. 7 Influence of mechanical damping on rotor response.

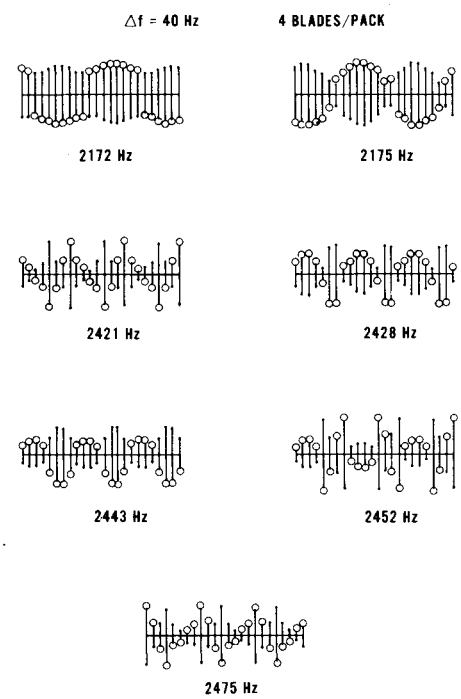

Fig. 9 Computed mode shapes for 24-bladed rotor with square frequency distribution.

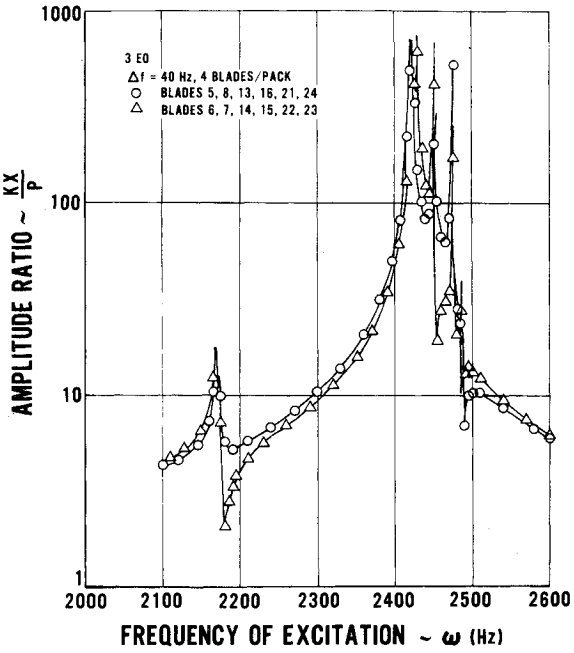

Fig. 10 Influence of blade location on response levels.

to that shown in Fig. 7 with an overstressing of 42% experienced by the same blade.

Bladed Disk with a Periodic Square Mistune Distribution (Packs of Different Sizes)

The arrangement of blades is shown in the insert to Fig. 8. A study is made of the effect of varying the pack size on the response to a 3E excitation. The results of these investigations are presented in Figs. 8–10. For a pack size of two, Fig. 8 shows that resonances are confined to the region close to the tuned wheel frequency, viz, 2438 Hz. However, as the size of the pack is increased to four blades, additional resonances are encountered at 2172 and 2175 Hz respectively. Analysis of the mode shapes of the rotor with the latter distribution (see Fig. 9) shows that these additional modes represent a splitting of a predominantly 3-diametral mode which is eliminated when the pack size is reduced in half. Although this example is far fetched because it is unlikely that blades of an actual rotor can be split into two discrete frequencies, it is shown that by rearranging the blades, one can eliminate certain resonances. The remaining modes of the analyzed rotor are characterized by periodic amplitude distributions whose period is twice that of the frequency distribution with no predominant diametral pattern.

To show that stress amplitudes are functions of both blade frequency and blade location, the 3E response is plotted in Fig. 10 for blades having a frequency of 2450 Hz. It may be noted that the blades experience essentially the same amplitudes at "off-resonance" frequencies and the blades equidistant from the midpoint of the pack have identical responses, and that amplitudes are extremely sensitive to excitation frequency changes in the neighborhood of the resonance frequencies.

Conclusions

The following conclusions are drawn based on a detailed study of the vibration analysis for the 24-bladed rotor with given mistune distributions. 1) Frequencies and mode shapes are in good agreement with the experimental results of Ref. 5. 2) Blades of a mistuned rotor appear to possess the same number of resonances at nearly the same frequencies. The latter are located in a band whose width depends upon the rotor characteristics and the mistune distribution. For the example studied here, the spread was calculated to be around 20% of the mean blade frequency (see Fig. 5). 3) Mistuning can cause higher stresses than those calculated on the basis of an ideally tuned rotor. The amount of overstressing depends on the frequency distribution and the deviation of blade frequencies from the mean value. 4) The blade experiencing the maximum stress level is not necessarily that of worst mistune. 5) Smooth mistune distributions do not necessarily imply lower vibration stresses.

References

[1] Wagner, J. T., "Coupling of Turbomachine Blade Vibrations through the Rotor," *Transactions of the ASME, Journal of Engineering for Power*, Vol. 89, Oct. 1967, pp. 502–513.

[2] Dye, R. C. F. and Henry, T. A., "Vibration Amplitudes of Compressor Blades Resulting from Scatter in Blade Natural Frequencies," *Transactions of the ASME, Journal of Engineering for Power*, Vol. 91, July 1969, pp. 182–188.

[3] Ewins, D. J., "The Effects of Detuning upon the Forced Vibrations of Bladed Disks," *Journal of Sound Vibration*, Vol. 9, 1969, pp. 65–79.

[4] Whitehead, D. S., "Effect of Mistuning on the Vibrations of Turbomachine Blades Induced by Wakes," *Journal of Mechanical Engineering Science*, Vol. 8, No. 1, March 1966, pp. 15–21.

[5] Ewins, D. J., "A Study of the Vibration Modes of a Bladed Turbine Wheel," *Conference on Vibrations in Rotating Systems*, Institution of Mechanical Engineers, London, Feb. 1972, pp. 170–184.

[6] Ehrich, F. F., "A Matrix Solution for the Vibration Modes of Non-Uniform Disks," *Transactions of the ASME, Journal of Applied Mechanics*, March 1956, pp. 109–115.